

# $\gamma$ -Radiation of Excited Nuclear Discrete Levels in Peripheral Heavy Ion Collisions

V.L.Korotkikh, K.A.Chikin

*E-mail: vlk@lav1.npi.msu.su*

Scobeltsyn Institute of Nuclear Physics, Moscow State University, 119899 Moscow,  
Russia

## Abstract

We study a new process of peripheral heavy ion collisions in which a nucleus is excited to the discrete state and then emits  $\gamma$ -rays. Large nuclear Lorentz factor allows to observe the high energy photons. On one hand it gives a significant background of  $\gamma$ -rays in the nuclear fragmentation region and on the other hand it can be used for the nuclear beam intensity monitoring by TOTEM CMS. We show that a two step process, in which at first the electron positron pair is produced by virtual photons of nucleus and then the electron (positron) excites the nucleus has large cross-section about 5 barn. The energy and angular distributions of the secondary photons emitted by nucleus in such process is calculated. The secondary photons have the energies up to 26 GeV and fly to the angles of a few hundred mikroradians along the beam direction for Ca-Ca collisions at LHC energies.

# $\gamma$ -RADIATION OF EXCITED NUCLEAR DISCRETE LEVELS IN PERIPHERAL HEAVY ION COLLISIONS

*V.L.Korotkikh, K.A.Chikin*

Scobeltsyn Institute of Nuclear Physics, Moscow State University, 119899  
Moscow, Russia. E-mail: vlk@lav1.npi.msu.su

## Abstract

We study a new process of peripheral heavy ion collisions in which a nucleus is excited to the discrete state and then emits  $\gamma$ -rays. Doppler effect at large nuclear Lorentz factor allows to observe the high energy photons. On one hand it gives a significant background of  $\gamma$ -rays in the nuclear fragmentation region and on the other hand it can be used for the nuclear beam intensity monitoring by TOTEM CMS. We show that a two stage process, in which at first the electron positron pair is produced by virtual photons of nucleus and then the electron (positron) excites the nucleus has large cross-section about 5 barn. The energy and angular distributions of the secondary photons emitted by nucleus in such process is calculated. The secondary photons have the energies up to 26 GeV and fly to the angles of a few hundred mikroradians along the beam direction for Ca-Ca collisions at LHC energies.

## 1 Introduction

Two photon physics calls very much attention. It includes the effects of coherent photon interactions for nuclear peripheral collisions. The ions do not interact directly with each other and move on essentially undisturbed in the beam direction. The only possible interaction are therefore due to the long range electromagnetic processes. Its cross-section is proportional for symmetrical case ( $Z_1 = Z_2 = Z$ ) to  $(\alpha Z)^4$ , where  $Z$  is the charge of each ion  $A_Z$ . Such processes have place at large distance between nuclei at  $b > 2R_A$ , where  $b$  is an impact parameter of two nuclear centers.

The selection of peripheral collisions is a very difficult experimental problem. In the present work we suggest to study the excitation of nucleus, which gives  $\gamma$ -rays for triggering the peripheral processes. The experiment has to measure the secondary photons emitted by nuclear excited discrete states. In this case the nucleus preserves its proton and neutron numbers. We can select such kind of events “event by event”. We also consider the grazing AA collisions in which the secondary photons are emitted. One more source of photons is  $\pi^0$  production in peripheral collisions. The other is the excitation of nucleus by strong and electromagnetic interactions. We study a two stage process, in which at first the electron positron pair is produced by virtual photons of nucleus and then the electron (positron) excites the nucleus. Such process without any additional particle production can be used for the nuclear beam monitoring.

There are many theoretical works in which the process of two virtual photon fusion in the peripheral AA collision

$$\gamma^* + \gamma^* \rightarrow M \tag{1}$$

is studied, where  $M$  is a particle system or a resonant state. The fusion of photons can produce the different particles from  $\mu^\pm$ ,  $\tau^\pm$  leptons to Higgs bosons [1, 2, 3, 4, 5]. The full list of references can be found in the recent reviews [1, 2, 3].

We considered three inclusive processes in our previous work [5], in which  $\pi^0$ -mesons are produced in grazing  $AA$  collisions ( $b > 2R_A$ ). The virtual photon fusion of nuclear electromagnetic fields

$$\gamma^* + \gamma^* \rightarrow \pi^0 \quad (2)$$

can give us  $\pi^0$  at most in the central rapidity region and at small  $p_T < 75$  MeV. The photo-disintegration of nucleus

$$\gamma^* + A_Z \rightarrow \pi^0 + X \quad (3)$$

produces also  $\pi^0$ -mesons with large amount of nuclear fragments in the fragmentation region [6, 7]. The process of strong nuclear interaction by the tails of nuclear density at  $b > 2R_A$

$$A_Z + A_Z \rightarrow \pi^0 + X \quad (4)$$

produces  $\pi^0$ -meson in the whole rapidity region, but also together with the nuclear fragments and other particles in the fragmentation region. We showed that in order to distinguish the fusion process (2) against processes (3) and (4) it needs to use the strong  $p_T$  cut,  $p_T < 75$  MeV, for all produced particles. Additionally it is necessary to have an efficient trigger to distinguish photon-photon events from hadronic ones. G.Baur et al. [3] suggested to measure the intact nuclei after the interaction. Evidently it is impossible for CMS on LHC. The nuclei at such  $p_T$ -cut will emit in very small solid angle,  $\theta_A \leq 1$   $\mu$ rad, at LHC energies and fly into the beam pipe.

There are other suggestions to select the events with the peripheral  $AA$  collisions. One of them is to use the correlation between an impact parameter  $b$  and total transverse energy of particles  $E_T$  [8]. Other suggestion is the correlation of  $b$  and particle multiplicities [9]. But they are not “event by event” criteria of peripheral collision selection.

The pure electromagnetic processes of the electron-positron pair production [10, 11, 12, 13] and bremsstrahlung photons [14, 15, 16, 17] also studied. These processes are considered as a possible background contribution. The cross-section of  $e^+e^-$  pair production is huge. It is equal to 220 Kbar for Pb–Pb and 800 barn for Ca–Ca collisions at LHC energies. A direct bremsstrahlung from the heavy ion

$$A_Z + A_Z \rightarrow A_Z + A_Z + \gamma'_{BS} \quad (5)$$

is small [14, 15, 16]. Its cross-sections is proportional to factor  $Z^6\alpha^3/M_A^2$ . Authors of work [17] suggested to see the bremsstrahlung photons coming from the electrons and positrons, which are produced in peripheral ion collisions

$$A_Z + A_Z \rightarrow A_Z + A_Z + e^+e^- + \gamma'_{BS}. \quad (6)$$

The cross-section of the process has a scaling factor  $Z^4\alpha^5/m_e^2$ . So it is larger than the cross-section of process (5). We used the result of work [17] for Pb–Pb and got about 10 barn for Ca–Ca at LHC energies. The energies of bremsstrahlung photons are small,  $E_{\gamma'_{BS}} \leq 3$  MeV, and the angles are near  $\theta_{\gamma'_{BS}} = 1^\circ$ . So such small energy photons are not interesting for our aims.

In the present work we are studying a new process when a nucleus is excited to the discrete level by electron (positron) which is produced by the electromagnetic interaction of nuclei

$$A_Z + A_Z \rightarrow A_Z^* + A_Z + e^+e^- \quad (7)$$

and then the excited nucleus  $A_Z^*$  radiates the secondary photon

$$A_Z^* \rightarrow A_Z + \gamma'. \quad (8)$$

As a rule the energy of nuclear excitation is order a few MeV [18]. So the energy  $E_{\gamma'}^0$  of photon in the nucleus rest (NR) system in MeV scale becomes to be equal to a few ten GeV or more in the laboratory system (LS) at LHC energies. The polar angle  $\theta_{\gamma'}$  of the secondary photon is about a few hundred  $\mu\text{rad}$ . It makes the favorable conditions for the photon registration.

A source of secondary photons can be also the light or heavy mesons, for example  $\pi^0$ . We are interested in the fusion process (2) in which both nuclei preserve their  $A$  and  $Z$ . So we suggest to remove the events of the processes (3) and (4) by the help of the veto-detectors on nuclear fragments.

The same conclusion concerns the processes  $AA$  collisions by the double Pomeron-exchange (**P**) [19]

$$\mathbf{P} + \mathbf{P} \rightarrow \pi^0 + \mathbf{X} \quad (9)$$

in the case, when the nuclei destroy. If the nuclei don't destroy then we can use again  $p_T$ -cut. A calculation of PHOJET event generator [20] for Pomeron-exchange gives an average transverse momentum of about 450 MeV. So the process (2) will be dominant over the process (9) at  $p_T < 75$  MeV.

There are other competing processes, which are also the sources of secondary photons. The excitation of nucleus by the strong interaction

$$A_Z + A_Z \rightarrow A_Z^* + A_Z, \quad A_Z^* \rightarrow \gamma' + A_Z \quad (10)$$

in the peripheral nuclear collision at  $b > 2R$ . We'll show that its cross-section is smaller than one of the process (7). The second process is the electromagnetic excitation of one nucleus by a virtual photon of another nucleus

$$\gamma^* + A_Z \rightarrow A_Z^*, \quad A_Z^* \rightarrow \gamma' + A_Z. \quad (11)$$

It is clear that the cross-section of this process is on two orders smaller than the cross-section of previous process by the scaling factor  $\alpha$ .

Other processes, which can be the source of secondary photons, are the excitation of nucleus in continuum spectrum with the cascade transitions to lower nuclear states and with the emission of photons. Such processes have the large probability of particle decay,  $A^* \rightarrow (A-4) + {}^4\text{He}$ ,  $A^* \rightarrow (A-1) + \text{N}$ , if the excitation energy is higher than particle decay threshold [18]. We suggest to remove the contribution of these processes with the help of veto detectors on charge particles. We need also to exclude the secondary photon contribution of nuclear fragments in the photo-disintegration reactions

$$\gamma^* + A_Z \rightarrow A_1^* + A_2^* + \dots, \quad A_k^* \rightarrow \gamma + A_k. \quad (12)$$

Our estimation based on the calculations in work [6] by the help of the code RELDIS shows that the nuclear fragments fly under polar angles less than a few ten  $\mu\text{rad}$ ,  $\theta \leq 45 \mu\text{rad}$ . So the fragments don't hit the central detectors of CMS LHC. They can be remove either by the quadrupole lens or by the special detectors in the Roman pots of TOTEM [21].

The TOTEM CMS project plans to measure a proton recoil or the products of diffraction dissociation at small  $t$ ,  $0.02 < |t| < 0.7$  (GeV/c)<sup>2</sup>, which is correspond to small polar angles  $20 < \theta < 120$   $\mu$ rad respect to the beam direction. So the gamma radiation of the secondary photons of process (7) can be a significant background for nucleus-nucleus collisions. As it will be shown the cross-section of the process (7) is large,  $\sigma \approx 5$  barn, so very many secondary photons hit the detectors in Roman pots.

There are two application of the secondary photons in the process (7). The first is a possibility to use them for the nuclear beam intensity monitoring. This problem on RHIC BNL is settled by the help of neutron Zero Degree Calorimeter (ZDC) [22]. The beam crossing angle on RHIC is  $\theta_{cross} = 14$  mrad and ZDC measure neutrons in the region  $\Delta\theta = 6$  mrad. The beam crossing angle on LHC is very small,  $\theta_{cross} = 300$   $\mu$ rad. The problem of nuclear beam intensity monitoring is not settled up to now. So, the consideration of the process (7) for monitoring of nuclear beam on LHC is important.

The second application of the secondary photons concerns the selection of peripheral nucleus-nucleus collisions in processes like the next:

$$A_Z A_Z \rightarrow A_Z^* A_Z + e^+ e^- + M, \quad A_Z^* \rightarrow \gamma' + A_Z; \quad (13)$$

$$A_Z A_Z \rightarrow A_Z^* A_Z + M, \quad A_Z^* \rightarrow \gamma' + A_Z, \quad (14)$$

where  $M$  is the produced particle system. The total trigger requirements include following features: a signal in the medium rapidity region from  $\gamma^* \gamma^* \rightarrow M$  events, the absent of signals from charge particles in high rapidity region of nuclear fragmentation and the photon signal in Roman pots station. We don't calculate these processes in the present work. We study the angular and energy distributions of secondary photons in decay (8) for the process (7). The nuclei in the processes like (13) and (14) preserve its charge and nucleon number. It is a main condition of peripheral electromagnetic nuclear interactions (see the work [3] and our study in [5]).

## 2 Formalism

### 2.1 Secondary nuclear $\gamma$ -radiation

Let's see an  $\gamma'$ -radiation of the relativistic nucleus with Lorentz factor  $\gamma_A$  from discrete level

$$A^*(J^P, E_\gamma^0) \rightarrow A + \gamma'. \quad (15)$$

Let's the secondary  $\gamma'$  photon flights at angle  $\theta_{\gamma'}$  and energy  $E_\gamma^0$  in the nucleus rest (NR) system. Then we have

$$E_\gamma = \gamma_A E_\gamma^0 (1 + \cos \theta_{\gamma'}) \quad (16)$$

in the laboratory system (LS) and, consequently,  $E_\gamma \leq 2\gamma_A E_\gamma^0$ . So,

$$\left| \frac{dE_\gamma}{d\theta_{\gamma'}} \right| = \gamma_A E_\gamma^0 \cdot \sin \theta_{\gamma'}. \quad (17)$$

The angles in the laboratory and nuclear rest system are connected by

$$\tan \theta_\gamma = \frac{1}{\gamma_A} \frac{\sin \theta_{\gamma'}}{(1 + \cos \theta_{\gamma'})}. \quad (18)$$

So,

$$\frac{d\theta_{\gamma'}}{d\theta_{\gamma}} = \frac{2\gamma_A}{(1 + \gamma_A^2 \tan^2 \theta_{\gamma}) \cos^2 \theta_{\gamma}}. \quad (19)$$

The number of photons conserving gives us

$$f(E_{\gamma})dE_{\gamma} = f(\theta_{\gamma}')d\theta_{\gamma}'. \quad (20)$$

The angular distribution of the secondary photon is in LS

$$\frac{dP_{A^*}}{d\theta_{\gamma}}(\theta_{\gamma}) = f(\theta_{\gamma}')\frac{d\theta_{\gamma}'}{d\theta_{\gamma}} \quad (21)$$

and the energy secondary photon distribution is

$$\frac{dP_{A^*}}{dE_{\gamma}}(E_{\gamma}) = f(\theta_{\gamma}')\frac{d\theta_{\gamma}'}{dE_{\gamma}} = f(\theta_{\gamma}')\frac{\Theta(2\gamma_A E_{\gamma}^0 - E_{\gamma})}{\gamma_A E_{\gamma}^0 \sin \theta_{\gamma}'}, \quad (22)$$

where the function  $\Theta(x) = 1$ , if  $x \leq 0$ , and  $\Theta(x) = 0$ , if  $x > 0$ .

For the isotropical  $\gamma'$  photon distribution in NR system

$$f(\theta_{\gamma}')d\theta_{\gamma}' \cdot d\varphi_{\gamma}' = \frac{1}{4\pi} \sin \theta_{\gamma}' d\theta_{\gamma}' d\varphi_{\gamma}' \quad (23)$$

we got after the integration on  $\varphi_{\gamma}'$

$$\frac{dP_{A^*}}{d\theta_{\gamma}}(\theta_{\gamma}) = \frac{1}{2} \frac{\sin \theta_{\gamma}' \cdot d\theta_{\gamma}'}{d\theta_{\gamma}}, \quad (24)$$

$$\frac{dP_{A^*}}{dE_{\gamma}}(E_{\gamma}) = \frac{1}{2\gamma_A E_{\gamma}^0} \Theta(2\gamma_A E_{\gamma}^0 - E_{\gamma}). \quad (25)$$

For comparison the photon distribution of  $\pi^0$  decay is

$$\frac{dP_{\pi^0}}{dE_{\gamma}}(E_{\gamma}) = \frac{1}{\gamma_{\pi^0} m_{\pi^0}} \Theta(\gamma_{\pi^0} m_{\pi^0} - E_{\gamma}). \quad (26)$$

The angular photon distribution (24) written through an angle  $\theta_{\gamma}$  in LS is

$$\frac{dP_A^*}{d\theta_{\gamma}} = \frac{2 \cdot \gamma_A^2 \cdot \sin \theta_{\gamma}}{(1 + \gamma_A^2 \tan^2 \theta_{\gamma})^2 \cos^3 \theta_{\gamma}}. \quad (27)$$

## 2.2 Excitation of discrete nuclear level in quasi-elastic electron scattering

Let's follow an author of the detail work [23]. The cross-section of nuclear excitation by electron scattering

$$e + A \rightarrow e' + A^*(\lambda^P, E_{\gamma}^0) \quad (28)$$

is

$$\frac{d\sigma_{A^*}}{d\Omega'} = \sigma_M(q) F_{\lambda}^2(q). \quad (29)$$

Here we neglect nuclear recoil effect. The equation is valid in the NR system, where the electron has an energy  $\varepsilon_0$  and the transfer momentum is

$$q = \sqrt{2\varepsilon_0} \sin \frac{\Theta_{e'}}{2}, \quad (30)$$

where  $\Theta_{e'}$  is an scattering angle of the electron. The Mott's cross-section is

$$\sigma_M(q) = \frac{(Z_A Z_e)^2}{q^4} \varepsilon_0^2 = \left( \frac{Z_A Z_e}{2\varepsilon_0} \right)^2 \frac{1}{\sin^4 \frac{\theta_{e'}}{2}}. \quad (31)$$

The good approximation of experimental inelastic form-factor  $F_\lambda(q)$  is found in the work [15]

$$F_\lambda(q) = \frac{1}{Z_A} c_\lambda q^\lambda \left[ 1 - \beta \left( \lambda + \frac{3}{2} \right) + \frac{\beta}{4} (dq)^2 \right] e^{-(dq)^2/4}, \quad (32)$$

$$c_\lambda = \frac{N_\lambda \pi \sqrt{2\lambda + 1} d^{\lambda+3}}{2^{\lambda+1}}. \quad (33)$$

For example, parameters for the  $^{40}\text{Ca}^*(3^-, 3.74 \text{ MeV})$  are  $N_3 = 0.0496 \text{ fm}^{-3}$ ,  $d = 2.015 \text{ fm}$ ,  $\beta = 0.8$  at  $\lambda = 3$ .

We also need some kinematic formulae. Let the four-dimension vectors of electron and nucleus are

$$\begin{aligned} k_e &= (\varepsilon, p \sin \theta \cdot \cos \varphi, p \sin \theta \cdot \sin \varphi, p \cos \theta), \\ k_A &= (E_A, 0, 0, -p_A) \end{aligned} \quad (34)$$

in the laboratory system (LS) and

$$k_e' = (\varepsilon_0, \vec{p}_e'), k_A' = (m_A, 0) \quad (35)$$

in the nuclear rest system.

Then

$$\varepsilon_0 = \frac{1}{m_A} (\varepsilon E_A + p \cdot p_A \cos \theta), \quad (36)$$

$$q_{max}(\varepsilon_0) = \sqrt{2} \cdot \varepsilon_0, \quad (37)$$

where the angle  $\theta$  is an polar angle of electron in LS with the axes  $Z || \vec{p}_A$ .

The equation (36), (37) gives us the possibility to calculate the cross-section of quasi-elastic excitation electron scattering in the system of colliding nuclei.

### 2.3 Nuclear excitation by electron or positron in peripheral RIC

Let's see the two stage process (fig. 1)

$$A_Z + A_Z \rightarrow A_Z^* + A_Z + e^+ e^- \quad (38)$$

in which at first the pair  $e^+ e^-$  is produced by the virtual photons of nuclear electromagnetic field and then the electron or positron excites the nucleus.

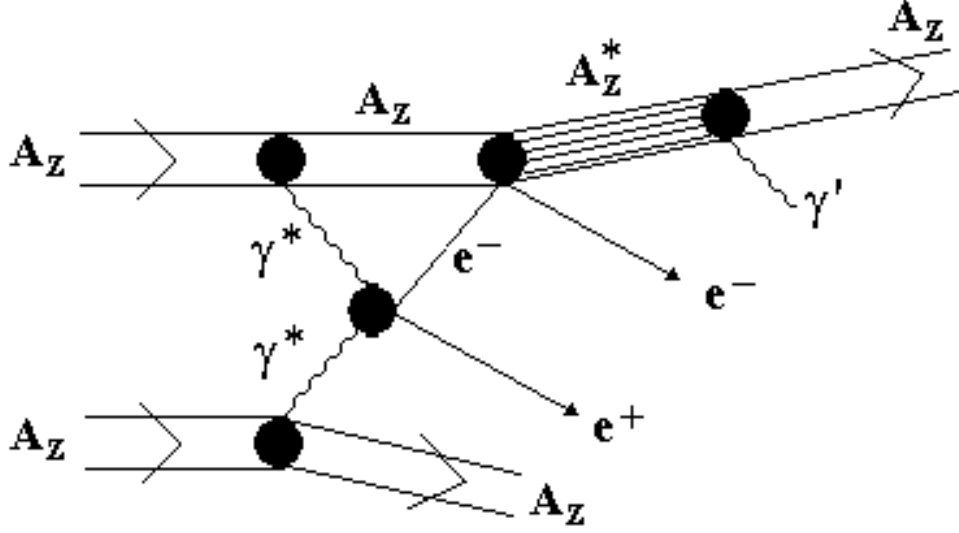


Figure 1:

Diagram of two stage process of nuclear excitation by electron (positron) produced by the virtual photon interaction in AA collision at LHC.

The authors of [10] showed in the double equivalent photon approximation, that the energy and angular electron (positron) distribution is

$$\frac{d\sigma_{AA}}{d\varepsilon d\Omega} = \frac{\alpha^2}{2} p \int_{\hat{E}/2}^{\infty} \frac{d\omega}{\omega^4} \frac{2\omega - \hat{E}}{\hat{E}^2} n(\omega) n\left(\frac{\omega \hat{E}}{2\omega - \hat{E}}\right) \cdot g(\omega, \theta), \quad (39)$$

where  $\omega$  is an energy of virtual photon,

$$\begin{aligned} \hat{E} &= \varepsilon + p \cos \theta, \\ \tilde{E} &= \varepsilon - p \cos \theta, \\ \varepsilon^2 &= p^2 + m_e^2, \\ g(\omega, \theta) &= \left\{ \frac{2\omega\omega' - m_e^2 + (\omega\omega' - m_e^2) \sin^2 \theta}{m_e^2 - (\omega\omega' - m_e^2) \sin^2 \theta} - \frac{2(\omega\omega' - m_e^2)^2 \sin^4 \theta}{[m_e^2 + (\omega\omega' - m_e^2) \sin^2 \theta]^2} \right\}, \\ \omega' &= \frac{\omega \tilde{E}}{2\omega - \hat{E}}. \end{aligned} \quad (40)$$

$$\begin{aligned} n(\omega) &= \frac{2}{\pi} Z_A^2 \alpha \left(\frac{c}{v}\right)^2 \left[ \xi K_0(\xi) K_1(\xi) - \frac{v^2 \xi^2}{2c^2} (K_1^2(\xi) - K_0^2(\xi)) \right], \\ \xi &= \frac{\omega R_{min}}{\gamma v}. \end{aligned} \quad (41)$$

Now we convolve two cross-section (39) and (29)

$$d\sigma_{AA^*} = \int d\varepsilon d\Omega \frac{d\sigma_{AA}}{d\varepsilon d\Omega}(\varepsilon, \theta) \cdot \frac{1}{\sigma_M(q)} \frac{d\sigma_{A^*}}{dq^2}(q) dq^2. \quad (42)$$



So, the cross-section of process (38) is

$$\begin{aligned}
d\sigma_{AA^*} &= 2\pi^2 \cdot \alpha^2 \int_{\hat{E}/2}^{\infty} d\omega \int_{m_e}^{\infty} d\varepsilon \int d\cos\theta \int d\cos\theta_{e'} \times \\
&\times p(\varepsilon) \frac{2\omega - \hat{E}}{\omega^4 \tilde{E}^2} n(\omega) n(\omega') \cdot g(\omega, \theta) \cdot (F_\lambda(q))^2.
\end{aligned} \tag{43}$$

After the electro-excitation of nucleus in LS when at high energies and small angle scattering of electron the nucleus recoil practically conserve its direction. So, the angular and energy distribution of secondary photon are

$$\frac{d\sigma_{AA^*}}{d\theta_{\gamma'}}(\theta_{\gamma'}) = d\sigma_{AA} \cdot \frac{dP_{A^*}}{d\theta_{\gamma'}}(\theta_{\gamma'}), \tag{44}$$

$$\frac{d\sigma_{AA^*}}{dE_{\gamma'}}(E_{\gamma'}) = d\sigma_{AA} \cdot \frac{dP_{A^*}}{dE_{\gamma'}}(E_{\gamma'}), \tag{45}$$

where  $d\sigma_{AA}$  is given by formula (43). The functions  $dP_{A^*}/d\theta_{\gamma'}$  and  $dP_{A^*}/dE_{\gamma'}$  depend on angular distribution of  $\gamma'$  photon in NR system. For the isotropic  $\gamma'$  distribution they are given by formula (24) and (25).

## 2.4 Nuclear excitation by the strong interaction in peripheral RIC

Let's consider process of heavy ion strong interaction in which one of nucleus is excited to a discrete level

$$A_1 + A_2 \rightarrow A_1^* + A_2. \tag{46}$$

Our task is to made an estimation of the cross-section in the peripheral collisions at  $b > (R_1 + R_2)$ .

Let's write the differential cross-section for the elastic scattering  $A_1 + A_2 \rightarrow A_1 + A_2$ , neglecting the distortion effects [24],

$$\frac{d\sigma_{A_1 A_2}}{dq^2} = \frac{d\sigma_{NN}}{dq^2}(q^2) |A_1 A_2 S_{A_1}(\vec{q}) S_{A_2}(-\vec{q})|^2. \tag{47}$$

Here  $S_A(\vec{q})$  is a nuclear form-factor, which is equal to unit at  $q = 0$ ,  $S_A(0) = 1$ . We can approximate it by the simple way

$$S_{A_i}(q) = e^{-B_{A_i} q^2/2}. \tag{48}$$

For the nucleon-nucleon scattering we use a standard form (see, for example, [2]) of the cross-section

$$\frac{d\sigma_{NN}}{dq^2}(q^2) = \left| \frac{\sigma_{tot}(NN)}{4\sqrt{\pi}} e^{-B_{NN} q^2/2} \right|^2. \tag{49}$$

We recalculate the energy of  $A + A$  collision at LHC with  $\gamma = 3500$  to the rest system of nuclear, where  $\gamma_A = 2\gamma^2 - 1$ . It gives us the value of  $NN$ -collision at rest system of nucleon  $E_p = 2.5 \cdot 10^7$  GeV. Then we use a good approximation of existing  $\bar{p}p$  data at  $\sqrt{s_{pp}} < 540$  GeV from work [25]. We got the values  $\sigma_{tot}(NN) \approx 100$  mb and  $B_{NN} \simeq 20$  GeV<sup>-2</sup> for the parameters in (49) at LHC energies.

For elastic scattering we can write the form-factor  $S_A(\vec{q})$  as

$$S_A(q) = 2\pi \int_0^\infty b db J_0(qb) T_A(b), \quad (50)$$

$$T_A(b) = \int_{-\infty}^\infty dz \rho_A(\vec{b}, Z),$$

where  $J_0(qb)$  is a Bessel function and  $\rho_A(\vec{b}, Z)$  is the nuclear density. The form (48) corresponds to Gaussian form of nuclear density. We have a simple form for  $T_A(b)$  with the parameterization (48)

$$T_A(b) = \frac{1}{2\pi B_A} e^{-b^2/(2B_A)}. \quad (51)$$

So, a transition to the peripheral collisions will be the integral (50) in the region  $b > R$

$$S_A(q, R) = 2\pi \int_R^\infty b db J_0(qb) T_A(b). \quad (52)$$

An amplitude of the proton inelastic scattering with the nuclear excitation to the state with spin  $\lambda$  and projection  $\mu$  in the same approximations is

$$\mathcal{F}_{pA^*}(\vec{q}) = A \cdot f_{NN}(\vec{q}) F_{\lambda\mu}(\vec{q}), \quad (53)$$

where

$$F_{\lambda\mu}(\vec{q}) = \int d^3\vec{r} e^{i\vec{q}\vec{r}} \rho_{\lambda\mu}(\vec{r}). \quad (54)$$

The transition nuclear density is

$$\rho_{\lambda\mu}(\vec{r}) = \frac{1}{A} \langle \lambda\mu | \sum_{j=1}^A \delta(\vec{r} - \vec{r}_j) | 00 \rangle. \quad (55)$$

It is simpler to show that  $F_{\lambda\mu}(q)|_{q \rightarrow 0} \sim q^\mu$ . Let's define an inelastic nuclear form-factor  $S_{A^*}^{(\lambda)}(q)$  by equation

$$(S_{A^*}^{(\lambda)}(q))^2 = \sum_{\mu} |F_{\lambda\mu}(\vec{q})|^2. \quad (56)$$

If we suppose that the state with  $\mu = \lambda$  is dominant, we can approximate an inelastic form-factor  $F_\lambda(q)$  by simple function (32). This form coincides with form-factor from inelastic electron scattering [22]. Let's make the approximation that a charge and nucleon transition densities are the same. Then we take the parameters of inelastic form-factor for  $^{40}\text{Ca}^*(\lambda\mu)$  from the work [23] and renormalized the form-factor to  $\frac{Z_A}{A}$

$$S_{A^*}^{(\lambda)}(q) = \frac{Z_A}{A} F_\lambda(q). \quad (57)$$

The Fourier transformation, which is analogy to (52), can be written in peripheral collisions with the excitation of nuclear level  $\lambda$  at  $b > R$  as

$$S_{A^*}^{(\lambda)}(q, R) = 2\pi \int_R^\infty b db J_\lambda(qb) T_{A^*}^{(\lambda)}(b), \quad (58)$$

where the function  $T_{A^*}^{(\lambda)}(b)$  can be calculate by the inverse Fourier transformation from  $S_{A^*}^\lambda(q)$  to  $T_{A^*}^\lambda(b)$

$$T_{A^*}^{(\lambda)}(b) = \frac{1}{2\pi} \int_0^\infty q dq J_\lambda(qb) S_{A^*}^{(\lambda)}(q). \quad (59)$$

We can calculate (59) analytically with the form-factor parameterization (57), which gives us

$$T_{A^*}^{(\lambda)}(b) = \frac{1}{A} \frac{c_\lambda}{2} \left[ 1 - \beta \left( \lambda + \frac{3}{2} \right) + \beta \left( \frac{b}{d} \right)^2 \right] \left( \frac{4}{d^2} \right)^{\frac{\lambda+2}{2}} \left( \frac{b^2}{d^2} \right)^{\frac{\lambda}{2}} e^{-\frac{b^2}{d^2}}. \quad (60)$$

So, the final formulae of cross-section of process (46) for the equal nuclei  $A_1 = A_2$  will be

$$\frac{d\sigma_{A_1^* A_2}}{dq^2} = \frac{d\sigma_{NN}}{dq^2}(q^2) |A_1 A_2 S_{A_1^*}^{(\lambda)}(\vec{q}, R) \cdot S_{A_2}(-\vec{q}, R)|^2. \quad (61)$$

The energy and angular distribution of the secondary photon are the convolutions:

$$\frac{d\sigma_{A_1^* A_2}}{dE_{\gamma_1'}} = \int d^2 q \frac{d\sigma_{A_1^* A_2}}{dq^2}(q) \frac{dP_{A_1^*}}{dE_{\gamma_1'}}(E_{\gamma_1'}, \theta_{A_1^*}); \quad (62)$$

$$\frac{d\sigma_{A_1^* A_2}}{d\theta_{\gamma_1'}} = \int d^2 q \frac{d\sigma_{A_1^* A_2}}{dq^2}(q) \frac{dP_{A_1^*}}{d\theta_{\gamma_1'}}(|\theta_{\gamma_1'} - \theta_{A_1^*}|). \quad (63)$$

For symmetrical case  $A_1 = A_2 = A$  and for small angles

$$\theta_{A^*} = \frac{q}{p_A}. \quad (64)$$

### 3 Energy and angular of the secondary photon distributions

Here we consider three peripheral processes which give us the secondary photons. All three processes preserve the charge  $Z$  and nuclear number  $A$  of nucleus. The nucleus is excited and then emits the photons in the processes (7) and (10). The  $\pi^0$ -meson, produced by the virtual photon fusion, decays two photons in the third process (2).

Let's see the kinematic dependence of the photon energy  $E_\gamma$  on angle  $\theta_\gamma$  in LS (fig. 2). We take for our calculation the nucleus  $^{40}\text{Ca}$ . The beam luminosity for this ion at LHC is rather large  $L = (2 - 4) \cdot 10^{30} \text{ cm}^{-2} \text{ s}^{-1}$  (see the estimations in [2]). The characteristics of Ca discrete level are well known [18]. In fig. 2 we use five strongly excited levels by electrons [23] between which the level  $\lambda^P = 3_1^-$ ,  $E_\gamma^0 = 3.74$  MeV has the most intensity of excitation.

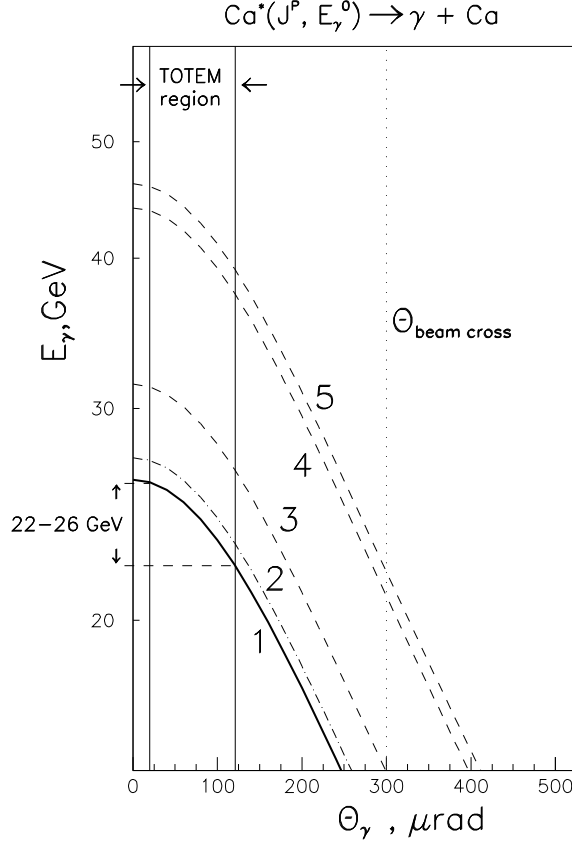


Figure 2: Kinematic dependence between energy and polar angle of photon emitted by the relativistic nuclei  $\text{Ca}^*(J^P, E_\gamma^0)$ . The lines correspond to the discrete excited levels: 1)  $3_1^-$ , 3.74 MeV, 2)  $2_1^+$ , 3.90 MeV, 3)  $5_1^-$ , 4.49 MeV, 4)  $3_2^-$ , 6.29 MeV, 5)  $3_3^-$ , 6.59 MeV. Vertical lines show the TOTEM region of angle  $20 \mu\text{rad} \leq \theta < 120 \mu\text{rad}$  and the angle of beam crossing at LHC.

The fig. 2 demonstrates that the energy  $E_\gamma$  falls quickly with the angle  $\theta_\gamma$  at  $\gamma_A = 3500$ . The energy  $E_\gamma$  is a few ten GeV in the solid angle  $\theta < \theta_{crossing\ beam}$ . The more intensity excitation level  $3^-$  gives the secondary photons with the energies  $22 \div 26$  GeV in the TOTEM measurable region of angles.

The fig. 3 shows the cross-sections (44) and (45) of two stage process (7) of the excitation of nucleus Ca by electron (positron), produced by the virtual photon interaction (see the section 2.3). The angular distribution of the secondary photons in NR system supposed to be flat because we average over all initial directions of electrons which excite the nucleus (see (42)). So the energy distribution (fig. 3a) is uniform. The level  $3^-$ ,  $E_\gamma^0 = 3.74$  MeV gives the most contribution to the sum of angle distributions over 5 levels in fig. 3b. The maximum of the angle distribution is at  $\theta_\gamma = 150 \mu\text{rad}$ .

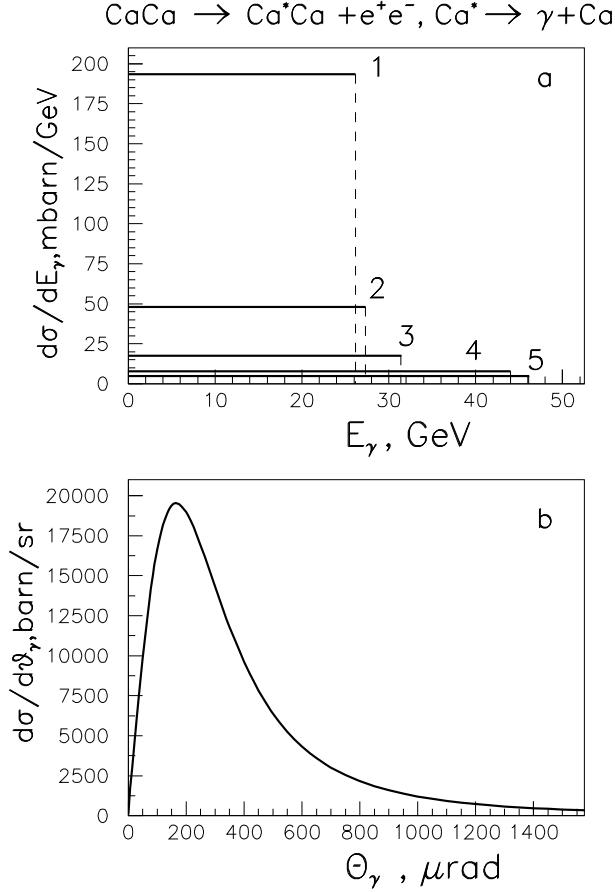


Figure 3: Energy and angular distribution of secondary photons in the process  $\text{Ca Ca} \rightarrow \text{Ca}^*(J^P, E_\gamma^0) \text{Ca} + e^+e^-, \text{Ca}^* \rightarrow \gamma + \text{Ca}$ . a) Photon energy distribution, numbers 1, 2,  $\dots$ , 5 corresponds nuclear levels (see fig. 1), b) Photon angular distribution for sum over all levels.

The integral cross-section of two stage process (7) is equal to  $\sigma_1 = 5.1$  barn at  $R_{min} = 1/m_e = 386$  fm. For the TOTEM angle region it is 16% of  $\sigma_1$  and for the region up to  $\theta_{crossing\ beam} = 300 \mu\text{rad}$  it is 56% of  $\sigma_1$ . The cross-section  $\sigma_1$  is large because the cross-section of the first stage  $\gamma^*\gamma^* \rightarrow e^+e^-$  is rather large. It is equal for Ca Ca collision to 842 barn at LHC energies.

The cross-section of the second process (10) in which the nucleus is excited by strong peripheral nuclear interaction is more less ( $\sigma_2 = 0.1$  mbarn) than the first one (fig. 4). We calculate this cross-section (57) with the rough approximation. We neglect the absorption effects of nucleus-nucleus interactions. So we got the upper estimation. We supposed also that the photon angular distribution in NR system is flat. The calculations are carried out at  $R_A = 1.2A^{1/3}$  fm and at  $b > R_A$  for each nucleus (see section 2.4). We use the values  $\sigma_{tot}(NN) = 100$  mbarn and  $B_{NN} = 20 (\text{GeV}/c)^{-2}$  at LHC energies.

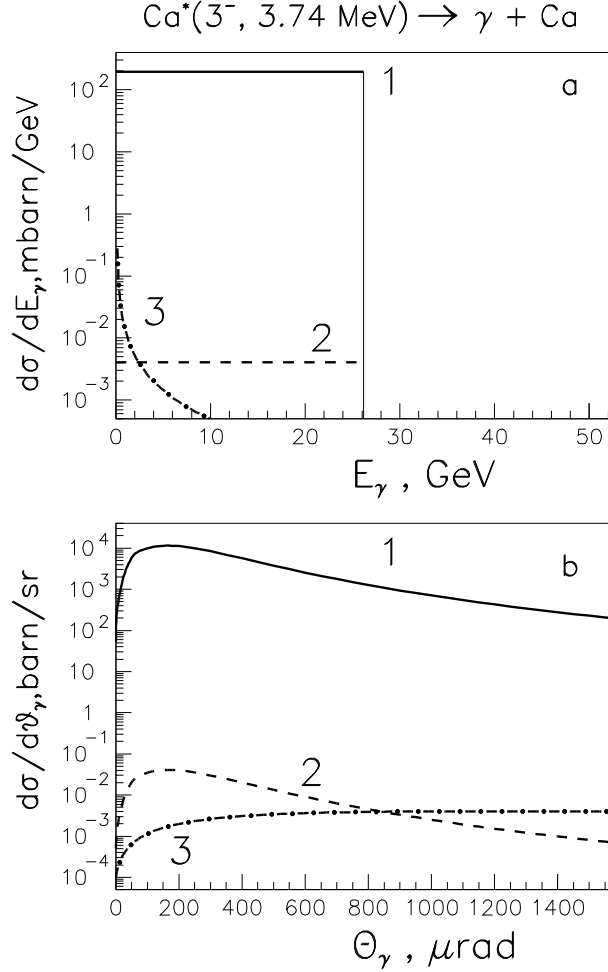


Figure 4: Comparison of energy (a) and angular (b) distribution of secondary photons for three peripheral processes: 1. The nuclear excitation by electron (positron), produced by electromagnetic interaction. 2. The excitation by strong peripheral interaction at  $b > 2R_A$ . 3. The fusion of virtual nuclear photons to  $\pi^0$  and its decay  $\pi^0 \rightarrow 2\gamma$ .

The distributions of the third process (2) of photon fusion to  $\pi^0$ ,  $\gamma^*\gamma^* \rightarrow \pi^0$  for Ca Ca collisions was calculated by the same way as in our previous work [5] for Pb Pb collisions. The cross-section of this process is also small ( $\sigma_3 = 0.19$  mbarn) compared with the two stage cross-section. The energy distribution (fig. 4a) of photons from  $\pi^0$  decay has a peak at  $E_\gamma = 0$  because we take into account  $\pi^0$  at any direction of its flying. The angular distribution has a very different form dependence compared with the photon angular distribution of nucleus radiation (fig. 4b).

## 4 Conclusions

We have presented the energy and angular distribution of the secondary photons from nuclear radiation in the peripheral ultrarelativistic  $AA$  collisions at LHC energies. The two stage process of nuclear excitation by electron (positron) produced by the virtual photon interaction has a large cross-section ( $\sim 5$  barn) and the specific angular distribution of the secondary photons. The  $\gamma$ -radiation of such nuclei can be measured by TOTEM installation in Roman pots at angles  $\sim 100$   $\mu\text{rad}$  and at energies  $\sim 20$  GeV for Ca Ca collision.

So, the high energy  $\gamma$ -radiation in peripheral collisions will be a significant background in the nuclear fragmentation region about  $10^6$  photon/sec for Ca–Ca collisions.

The secondary  $\gamma$ -radiation of nuclei can be used for the beam intensity monitoring which is very difficult problem for nuclear beam. But at first it is necessary to fulfill the preliminary measurements of such radiation intensity in a special experiment in order to verify the parameter  $R_{min}$  of nuclear electromagnetic interaction.

At last, the secondary nuclear photons can be a good signal for triggering the processes like (13) or (14) with meson system, produced in central rapidity region. Total trigger have to be a signal in the central rapidity region, the absent of signals from charge nuclear fragments in nuclear fragmentation region and the high energy photon signal in Roman pots detectors.

Authors are very grateful L.I. Sarycheva and I.A.Pshenichnov for the useful and fruitful discussions.

## References

- [1] F.Krauss, M.Greiner and G.Soft, Prog. Part. Nucl. Phys. **39**, 503 (1977).
- [2] G.Baur, K.Hencken, D.Trautmann, J. Phys. **G24**, 1657 (1998).
- [3] G.Baur, K.Hencken, D.Trautmann, S.Sadovsky and Yu.Kharlov, CMS Note 1998/009, hep-ph/9904361.
- [4] S.Klein and J.Nystrand, Phys. Rev. **C60**, 014903 (1999).
- [5] K.A.Chikin et al., Eur. Phys. J. **A8**, 537 (2000).
- [6] I.A.Pshenichnov et al. Phys. Rev. **C60**, 044901 (1999).
- [7] I.A.Pshenichnov et al. Phys. Rev. **C57**, 1920 (1998).
- [8] V.Emel'yanov, A.Khodirov, S.Klein and R.Vogt, LBNL-40398, 1997.
- [9] J.Nystrand and S.Klein, LBNL-42524, 1998, nucl-ex/9811007.
- [10] N.Baron, G.Baur, Phys. Rev. **D46**, R3695 (1992).
- [11] M.J.Rhoades-Brown, J.Weneser, Phys. Rev. **A44**, 330 (1991).
- [12] M.C.Güclü et al. Phys. Rev. **A51**, 1836 (1995).
- [13] A.Alscher et al. Phys. Rev. **A55**, 396 (1997).
- [14] C.A.Bertulani and G.Baur, Phys. Rep. **163**, 299 (1988).
- [15] H.Meier et al. Eur. J. Phys. J. **C2**, 741 (1998).
- [16] S.Jeon and J.Kapusta, A.Chikhanian, J.Sandweiss, nucl-th/9806047.
- [17] K.Hencken, D.Trautmann and G.Baur, nucl-th/9903019.
- [18] P.M. Endt et al., Nucl. Phys. **A633**, 1 (1998).
- [19] S.U.Chung, D.P.Weygand and H.J.Willutzki, Preprint BNL-QGS-02-91.
- [20] R.Engel et al. Z. Phys. **C74**, 687 (1997).
- [21] W.Kienzle et al., TOTEM, Letter of Intent, CERN/LHCC/ 97-49, 1997.
- [22] C.Adler, A.Denisov, E.Garcia, M.Mureau, H.Stroebele, S.White, nucl-ex/0008005.
- [23] I.S.Gulkarov, Fis. Elem. Chast. At Nucl., **19**, 345 (1998).
- [24] V.L.Korotkikh, I.P.Lokhtin. Sov. J. Nucl. Phys. **56**, 1110 (1993).
- [25] K.Goulios. Comments Nucl. Part. Phys. **17**, 177 (1987).